ACS Catalysis

Letter

pubs.acs.org/acscatalysis

Heterogeneous Catalyst for the Selective Oxidation of Unactivated Hydrocarbons Based on a Tethered Metal-Coordinated Cavitand

Junghyun Hong, Katherine E. Djernes, Ilkeun Lee, Richard J. Hooley, and Francisco Zaera*

Department of Chemistry, University of California, Riverside, Riverside, California 92521, United States

Supporting Information

ABSTRACT: A new selective hydrocarbon oxidation heterogeneous catalyst has been developed by tethering an iron-coordinated cavitand to the surfaces of a SBA-15 mesoporous material. The resulting material was shown to catalyze the oxidation of cyclic hydrocarbons at room temperature and to be quite robust and easily recyclable. The role of the cavitand scaffold is to prevent the catalytic Fe ions from interacting directly with the silica surface and to provide a controlled environment for reversible redox catalysis. An induction period is required for the activation of the catalyst, during which a change in coordination of the iron ions to the tethered cavitand takes place.

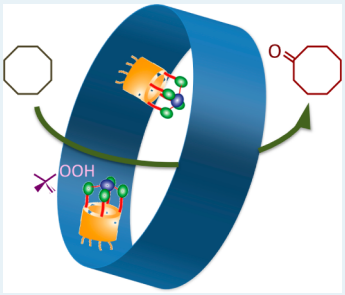

KEYWORDS: *hydrocarbon oxidation, click chemistry, tethering, cavitand, iron, heterogeneous catalyst*

The selective C−H oxidation of unactivated hydrocarbons is still one of the greatest challenges in catalysis.[1] Perhaps the most promising approach has been the use of biomimetic structures in which metal ions, Fe ions in particular, are coordinated to organic frameworks that emulate the structure of the active site of enzymes.[2−4] However, the effectiveness of those homogeneous catalysts is sometimes limited by their low solubility in specific solvents, their potential decomposition under oxidation conditions, and/or the need to separate them from the products after the reaction is completed. Heterogeneous catalysts are simpler and more robust, but the best of those developed to date require relatively high temperatures to operate and generally show poor selectivity.[5−7]

Here, we report on the performance of a heterogeneous catalyst made by tethering an iron-coordinated cavitand catalyst previously developed in our laboratory[8,9] to a SBA-15 mesoporous solid. Cavitands have been shown to coordinate Fe(II) ions, allowing solution-phase C−H oxidation of unactivated hydrocarbons in mild, aqueous conditions.[8,9] They are also well suited for use as solid surface-mounted scaffolds. In contrast, other known solution-phase biomimetic C−H oxidation catalysts are unsuited for surface attachment due to both the synthetic challenges in their derivatization and the fact that altering the ligand scaffold dramatically affects the catalytic activity of the system. Our new system proved to be active for the room-temperature C−H oxidation of some cyclic unactivated hydrocarbons, and also quite robust and easily recyclable.

The synthetic approach used for the buildup of the heterogeneous system is shown in Figure 1. Reaction of previously reported cavitand **1**[8] with 3-(triethoxysilyl)propyl isocyanate gave the tetrasilylated cavitand **2** in 38% yield. ^{1}H and ^{13}C NMR data for **2** is provided in Supporting Information Figures S2 and S3, respectively. Sonication of **2** with excess

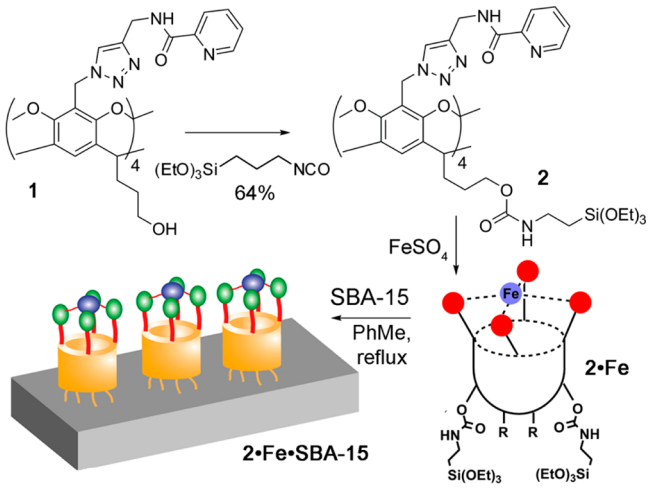

Figure 1. Synthesis and anchoring of cavitand catalysts on a SBA-15 silica support.

$FeSO_4$ in methanol afforded the coordination of Fe(II) ions to the four triazole groups at the cavitand rim to form **2·Fe** (^{1}H NMR provided in Supporting Information Figure S4). It is important to note that, in solution, **2** showed metal ion coordinating abilities very similar to **1**; this is a key property for the proposed catalysis. Attachment of the solution-phase catalyst **2·Fe** to the **SBA-15** mesoporous support was accomplished by refluxing in toluene.[10,11] Inactive tetrabromo cavitand **3** (Supporting Information Figure S1), a precursor in the synthesis of **1**, was also attached to the SBA-15 support

Received: June 21, 2013
Revised: August 7, 2013
Published: August 20, 2013

Table 1. Oxidation Activity of the Tethered (2·Fe·SBA-15) and Untethered (1·Fe) Fe-Coordinated Cavitand Catalysts[a]

	2·Fe·SBA-15			1·Fe[8,9]		
hydrocarbon	TON[b]	product distribution (%)		TON[c]	product distribution (%)	
fluorene	34	9-fluorenone (100)		7.4	9-fluorenone (100)	
cyclooctane	19	cyclooctanone (84)	1,4-cyclooctadione (16)	7.9	cyclooctanone (85)	1,4-cyclooctadione (15)
adamantane	0.3	1-adamantanol (98)	2-adamantanone (2)	5.7[d]	1-adamantol (61)	2-adamantanone (39)

[a]Reaction conditions (tethered catalyst): oxidant, *tert*-butyl hydroperoxide (10 equiv); solvent, 1:1 acetonitrile/water; cocatalyst, acetic acid (10 equiv); T = 300 K. [b]6 days. [c]1 day. [d]T = 333 K.

under identical conditions to provide an inactive control. More details of the synthesis are provided in the Supporting Information.

Tethering of the **2·Fe** system to the SBA-15 support was assessed by solid-state NMR. Bonding to the surface was identified by ^{29}Si cross-polarization magic-angle-spinning (CP/MAS) NMR (Supporting Information Figure S5). Spectra are provided for both the heterogeneous catalyst **2·Fe·SBA-15** and the tethered inactive cavitand **3**. In both cases, three new peaks are observed in the −45 to −70 ppm region as a result of the formation of the new Si−O−Si bonds,[12] mainly involving either one or two such bridging bonds per linker moiety, that is, per silane group (a quantitative analysis is provided in Supporting Information, Figure S6). The fact that no signal was seen around −40 ppm indicates derivatization of all four silane-terminated moieties in the cavitand precursor during tethering, whereas the large fraction of mono- and dihydroxo groups that remain on the derivatized surface points to a large degree of cross-polymerization of those groups. The integrity of the cavitand was corroborated by the ^{13}C CP/MAS NMR data (Supporting Information Figure S7).

In terms of the quantitation of the surface coverages of the active phase in the heterogenized catalyst, surface concentrations of tethered cavitands of approximately 5.4 and 1.6% (relative to the total number of exposed surface silicon atoms) were estimated for the free and iron-containing cavitands, respectively, on the basis of the relative areas of the ^{29}Si NMR peaks (uncorrected for differences in cross-polarization dynamics).[13,14] An independent quantitative measurement of the Fe ions on the surface, obtained by using a redox titration with $KMnO_4$[15] and assuming a density of OH groups on the surface of the SBA-15 of 1.1×10^{21} OH/g,[16] yielded a value of 2.3%. Contrast of these two measurements suggests an average Fe/cavitand ratio between 1 and 2 (2.3/1.6∼1.4), in line with our past observations of both mono- and di-iron coordination motifs with the homogeneous catalyst. Determination of this ratio after reaction is more difficult, but XPS measurements showed no changes in the surface concentration of the cavitand (Figure 4), and there were no indications of any iron loss during reaction either; it would appear that the overall Fe:cavitand ratio remains approximately constant during reaction. In addition, given the high overall values for the concentrations obtained for both the tethered cavitands and the iron ions, it can be concluded that the catalysts are tethered mainly on the inside walls of the pores of the SBA-15 solid: such mesoporous materials have quite high total areas, on the order of 600 m^2/g, and only a minute fraction of that corresponds to the outside surfaces.

The performance of catalyst **2·Fe·SBA-15** was tested next. Table 1 contrasts the results obtained for the oxidation of three hydrocarbons (fluorene, cyclooctane, and adamantane) with the **2·Fe·SBA-15** tethered catalyst versus the **1·Fe** untethered catalyst (like **2·Fe**, but without the silane linkers).[9] The reactions were performed by adding the catalyst and an excess of *tert*-butyl hydroperoxide (TBHP), the oxidant, to a solution of the hydrocarbon in 1:1 acetonitrile/water. Clearly, the **2·Fe·SBA-15** catalyst is still active after surface attachment. For instance, turnover numbers (TONs, in molecules converted per Fe ion) of 34 and 19 were measured after 6 days of reaction at room temperature for fluorene and cyclooctane, respectively. Its activity appears to be a little lower than that observed with the homogeneous counterpart, for which TON of 7.4 and 7.9 were obtained after only 1 day of reaction, respectively, but this could be due in part to the large uncertainty in the determination of the number of active sites on the surface, which makes a direct comparison of TONs valid only at a semiquantitative level. Moreover, the values in Table 1 are for initial TONs using fresh catalysts, and it was found that the activity of the tethered samples improves with time (see below). The main products with fluorene and cyclooctane are the corresponding ketones, as with the untethered catalyst **1·Fe**. Oxidation of adamantane is more challenging and requires slightly more elevated temperatures, and oxidation of acyclic alkanes such as *n*-octane or isooctane is basically undetectable. Overall, though, it appears that our cavitand-based catalyst is able to maintain its catalytic performance upon being tethered to the solid surface.

One advantage of the tethered catalyst is that it can be easily recycled. Figure 2 shows typical data for the performance of the same catalyst in successive oxidation runs with fluorene; the solid was recovered by centrifugation after washing to remove

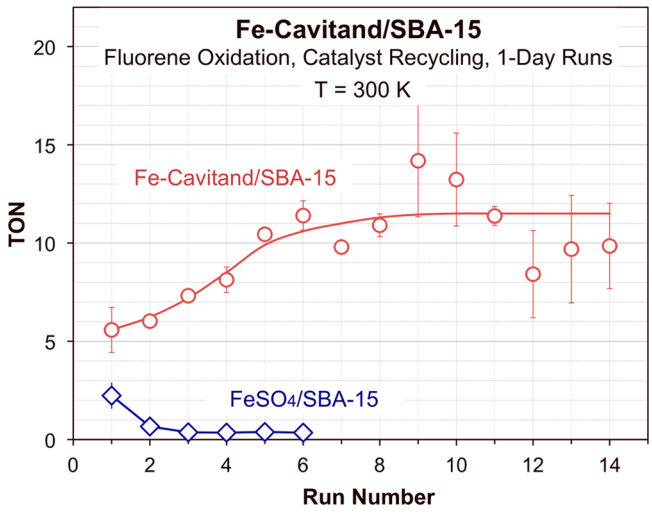

Figure 2. 2·Fe·SBA-15 catalytic activity for the oxidation of fluorene. Data are shown for a number of sequential runs performed with the same catalyst after filtering and adding fresh reaction mixtures. The results obtained with a reference catalyst obtained by impregnating the SBA-15 solid with $FeSO_4$ are also shown for reference.

dx.doi.org/10.1021/cs400471b | *ACS Catal.* 2013, 3, 2154−2157

all possible species from the liquid phase (including any potential leached iron, which would not be active for the oxidation reactions in solution anyway), and reused without further treatment. In addition to proving that the catalyst can be reused many times, the data also show that there is an induction period before the optimum activity is reached. Up to 14 runs could be performed without significant loss of activity. In contrast, although a catalyst prepared by simple impregnation of SBA-15 with a solution of Fe_2SO_4 did show some initial oxidation activity, that activity was lost after the first run. Clearly, the cavitand stabilizes the Fe ions during catalysis. More details on the conditions used for these experiments and more examples of recycling tests are provided in the Supporting Information (Figures S8 and S9).

Some clues on the molecular details associated with the performance of the **2·Fe·SBA-15** catalyst and the induction period required for optimum catalysis were obtained by using X-ray photoelectron spectroscopy (XPS). Typical Fe 2p, Fe 3p, and N 1s XPS spectra obtained for the catalyst at different stages of use are provided in Figure 3, and key results derived from a quantitative analysis of those data are summarized in Figure 4.

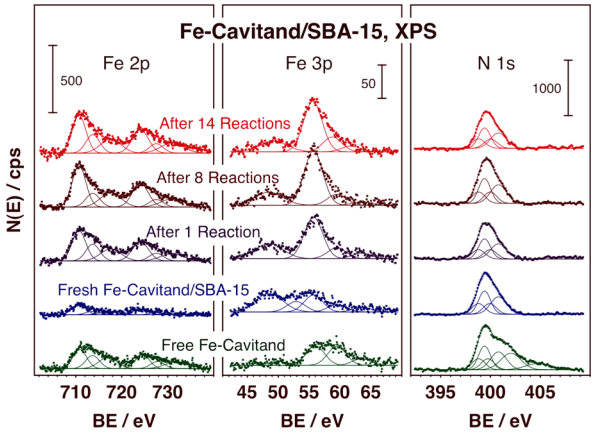

Figure 3. Fe 2p (left), Fe 3p (center), and N 1s (right) X-ray photoelectron spectra (XPS) for the **2·Fe·SBA-15** catalyst after different stages of use, from fresh (second traces from bottom) to following 14 catalytic cycles (top). Spectra for the free **2·Fe** are also included for reference (bottom).

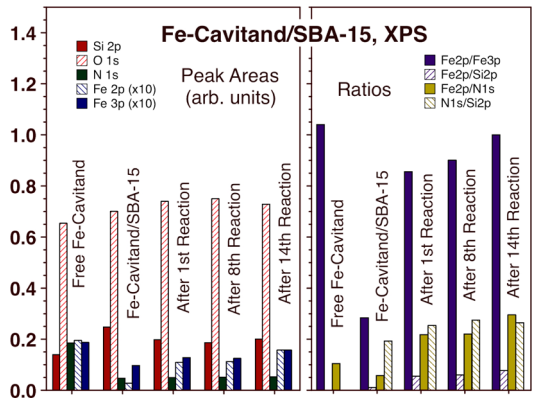

Figure 4. Quantitative analysis of the XPS data in Figure 3. The peak areas on the left panel are reported in arbitrary units, but were normalized by their sensitive factors[31] to provide the proper atomic ratios.

Several conclusions can be derived from analysis of the XPS data. For one, it is clear that the Fe XPS signals from the fresh **2·Fe·SBA-15** catalyst are quite weak, indicating that the Fe ions are most likely embedded deep below the organic layer. That situation reverses rapidly upon exposure to the reaction mixture, and strong signals appear in the spectra after only one catalytic run. Two additional observations are associated with this change, which we believe correlates with the induction period needed to fully activate the tethered catalyst. First, the Fe 2p/Fe 3p intensity ratio increases with catalyst usage. Because the mean free path of the 2p photoelectrons is shorter than that of the 3p counterparts (~2.5 vs 3.5 nm),[17] this means that the Fe atoms become more exposed over time. Second, the shape of the N 1s traces also changes as the catalyst is used, suggesting a change in the way the Fe ions coordinate to the cavitand. To better illustrate this point, the raw XPS traces were fit to a series of four Gaussian peaks, three of which were fixed at binding energies of 398.8, 400.0, and 400.8 eV for the nitrogen atoms in the pyridine,[18] ends of the triazole,[19] and carbamate[20] groups, respectively. The fourth peak, from the middle triazole nitrogen (which we propose coordinates the Fe ions),[8] was then adjusted to provide the best fit to the data. It was found that that peak drifts slightly, from 399.93 eV on the fresh catalyst to about 400.03 eV after extensive use (Supporting Information Figure S10). In contrast, the remaining N 1s XPS signals, as well as the C 1s XPS features (Supporting Information Figure S11), persist almost unmodified throughout the derivatization and catalytic use of the solid in terms of peak positions, peak shapes, and peak intensities, indicating that the cavitand is, indeed, incorporated into the mesoporous material and that it retains its molecular integrity all throughout the repeated exposures to the reaction mixtures. It is also noteworthy that the N 1s XPS trace for the unbound **2·Fe** catalyst is much more complex than those from the **2·Fe·SBA-15** tethered catalyst, suggesting perhaps more than one bonding mode for the iron ion in the former case. Fe bonding to the cavitand seems simpler on the tethered cavitand;[9] in solution, two coordination modes were observed for **1·Fe**, with either one or two Fe(II) ions.[8]

Another interesting observation deriving from the XPS data is the fact that the resting oxidation state of the iron ions in these catalysts appears to be Fe^{3+}, despite the use of Fe(II) salts in the initial coordination. This is indicated by the main peaks seen in the Fe $2p_{3/2}$ and 3p XPS traces, at 710.7 and 55.6 eV, respectively.[21,22] The XPS analysis has been performed ex-situ, after taking the samples from the reaction environment, but it would still be possible to detect other oxidation states, Fe^{2+} in particular, if those were present on these surfaces. Indeed, some signal from Fe^{2+}, at 709.5 and 54.1 eV in the Fe $2p_{3/2}$ and Fe 3p XPS traces, respectively, is seen with the fresh $FeSO_4$/SBA-15 reference catalyst (Supporting Information Figures S12 and S13). Those seem to be the ions that promote hydrocarbon oxidation with that reference sample, since they disappear irreversibly once the catalyst is spent. It would appear that one key role of the cavitand is to provide an environment in which the iron ions can undergo reversible redox chemistry; on the silica, the ions interact strongly with the surface and are not able to reversibly change their oxidation state.

Extracting information on the mechanistic details of this system are complicated by the two coordination geometries displayed by the **1·Fe** system,[9] but it can be said that the coordination sphere in both cases is similar to well-precedented nonheme iron oxidation catalysts inspired by the Rieske

dx.doi.org/10.1021/cs400471b | ACS Catal. 2013, 3, 2154−2157

dioxygenase structure.[3,23−30] The tetra-substituted Fe(II) species displays an octahedral geometry with the two empty coordination sites filled by donor solvent molecules. It is proposed that addition of aqueous *tert*-butyl hydroperoxide displaces some coordinated solvent molecules and forms the active intermediate Fe(V) oxo species that can insert oxygen into the C−H target bond, in a fashion similar to that which has been established with Fe(II) complexes of tetramine ligands.[3] This mechanism is further complicated in the tethered catalyst by the fact that the iron ions seem to require some repositioning before achieving optimum catalytic activity. It is not obvious at this stage of our research how the required rearrangement occurs, but what is clear is that it results in a better exposure of the iron ion to the solution of the reactants.

Our cavitand scaffold is more flexible than the catalysts described by White et al.[25,28,30] and Que et al.[23,27,29] and displays lower catalytic activity. For example, White's catalyst is capable of C−H bond oxidation with simple hydrocarbons at ambient temperature or below, whereas more challenging substrates such as cyclic hydrocarbons require slightly elevated temperatures with our catalyst. However, the advantage of our system is that it is possible to simply derivatize the cavitand base without altering the catalytic activity of the Fe−ligand scaffold. Although the original cavitand-based catalyst is not the most reactive C−H oxidation catalyst known, its derivatization allows immobilization on a solid surface, something that the other solution-phase catalysts are not capable of doing. Our resulting heterogeneous catalyst is perhaps the best hydrocarbon oxidation heterogeneous catalyst reported to date.

In summary, we have shown that it is possible to successfully tether an iron-coordinated cavitand to the surface of a mesoporous silica support. The activity of the resulting heterogeneous catalyst for the promotion of room-temperature oxidations of unactivated alkanes is qualitatively similar to that of the original homogeneous catalyst. The tethered catalyst does require initial activation via exposure to the reaction mixture, a process that leads to a change in the coordination of the iron ions to the cavitand. Nevertheless, the resulting catalyst is quite robust, retaining the molecular structure of the cavitand and showing minimum if any leaching of the iron ions, and easy to recycle. In more general terms, this example shows the promise of adding molecular structures to solid surfaces via covalent tethering, using simple "click" chemistry, as a way to achieve structurally complex sites in heterogeneous catalysts.

■ ASSOCIATED CONTENT

Supporting Information

Experimental details, NMR data, recycling data with fluorene, and XPS analysis. This material is available free of charge via the Internet at http://pubs.acs.org.

■ AUTHOR INFORMATION

Corresponding Author

*Email: zaera@ucr.edu.

Notes

The authors declare no competing financial interest.

■ ACKNOWLEDGMENTS

Funding for this project was provided by grants from the U.S. National Science Foundation (NSF, Grants CHE-1151773 to R.J.H. and CBET-1063595 to F.Z.). The XPS instrument used in this research was acquired with funds from NSF Grant DMR-0958796.

■ REFERENCES

(1) Cavani, F.; Teles, J. H. *ChemSusChem* **2009**, *2*, 508.
(2) Meunier, B. *Biomimetic Oxidations Catalyzed by Transition Metal Complexes*. Imperial College Press: London, 2000.
(3) Que, L.; Tolman, W. B. *Nature* **2008**, *455*, 333.
(4) Schröder, K.; Junge, K.; Bitterlich, B.; Beller, M. *Top. Organomet. Chem.* **2011**, *33*, 83−109.
(5) Punniyamurthy, T.; Velusamy, S.; Iqbal, J. *Chem. Rev.* **2005**, *105*, 2329.
(6) Dhakshinamoorthy, A.; Alvaro, M.; Garcia, H. *Catal. Sci. Technol.* **2011**, *1*, 856.
(7) Pradhan, S.; Bartley, J. K.; Bethell, D.; Carley, A. F.; Conte, M.; Golunski, S.; House, M. P.; Jenkins, R. L.; Lloyd, R.; Hutchings, G. J. *Nat. Chem.* **2012**, *4*, 134.
(8) Djernes, K. E.; Moshe, O.; Mettry, M.; Richards, D. D.; Hooley, R. J. *Org. Lett.* **2012**, *14*, 788.
(9) Djernes, K. E.; Padilla, M.; Mettry, M.; Young, M. C.; Hooley, R. J. *Chem. Commun.* **2012**, *48*, 11576.
(10) Corma, A.; Garcia, H. *Adv. Synth. Catal.* **2006**, *348*, 1391.
(11) Hong, J.; Lee, I.; Zaera, F. *Top. Catal.* **2011**, *54*, 1340.
(12) Krupczyńska, K.; Buszewski, B.; Jandera, P. *Anal. Chem.* **2004**, *76*, 226A.
(13) Caravajal, G. S.; Leyden, D. E.; Quinting, G. R.; Maciel, G. E. *Anal. Chem.* **1988**, *60*, 1776.
(14) Liu, C. C.; Maciel, G. E. *J. Am. Chem. Soc.* **1996**, *118*, 5103.
(15) Kolthoff, I. M.; Sandell, E. B.; Meehan, E. J.; Bruckenstein, S. *Quantitative Chemical Analysis*, 4th ed.; Macmillan: New York, 1969.
(16) Ide, M.; El-Roz, M.; De Canck, E.; Vicente, A.; Planckaert, T.; Bogaerts, T.; Van Driessche, I.; Lynen, F.; Van Speybroeck, V.; Thybault-Starzyk, F.; Van Der Voort, P. *Phys. Chem. Chem. Phys.* **2013**, *15*, 642.
(17) Seah, M. P.; Dench, W. A. *Surf. Interface Anal.* **1979**, *1*, 2.
(18) Ding-Bo, W.; Bao-Hua, C.; Bing, Z.; Yong-Xiang, M. *Polyhedron* **1997**, *16*, 2625.
(19) Stenehjem, E. D.; Ziatdinov, V. R.; Stack, T. D. P.; Chidsey, C. E. D. *J. Am. Chem. Soc.* **2013**, *135*, 1110.
(20) Böcking, T.; Kilian, K. A.; Hanley, T.; Ilyas, S.; Gaus, K.; Gal, M.; Gooding, J. J. *Langmuir* **2005**, *21*, 10522.
(21) Descostes, M.; Mercier, F.; Thromat, N.; Beaucaire, C.; Gautier-Soyer, M. *Appl. Surf. Sci.* **2000**, *165*, 288.
(22) Yamashita, T.; Hayes, P. *Appl. Surf. Sci.* **2008**, *254*, 2441.
(23) Chen, K.; Que, L., Jr. *J. Am. Chem. Soc.* **2001**, *123*, 6327.
(24) Abu-Omar, M. M.; Loaiza, A.; Hontzeas, N. *Chem. Rev.* **2005**, *105*, 2227.
(25) Chen, M. S.; White, M. C. *Science* **2007**, *318*, 783.
(26) Gómez, L.; Garcia-Bosch, I.; Company, A.; Benet-Buchholz, J.; Polo, A.; Sala, X.; Ribas, X.; Costas, M. *Angew. Chem., Int. Ed.* **2009**, *48*, 5720.
(27) Mukherjee, A.; Martinho, M.; Bominaar, E. L.; Münck, E.; Que, L. *Angew. Chem., Int. Ed.* **2009**, *48*, 1780.
(28) Bigi, M. A.; Reed, S. A.; White, M. C. *Nat. Chem.* **2011**, *3*, 216.
(29) England, J.; Guo, Y.; Van Heuvelen, K. M.; Cranswick, M. A.; Rohde, G. T.; Bominaar, E. L.; Münck, E.; Que, L. *J. Am. Chem. Soc.* **2011**, *133*, 11880.
(30) Bigi, M. A.; Reed, S. A.; White, M. C. *J. Am. Chem. Soc.* **2012**, *134*, 9721.
(31) XPS Atomic Sensitivity Factors versus Atomic Number. In *Practical Surface Analysis*; Briggs, D., Seah, M. P., Eds.; John Wiley and Sons: Chichester, UK, 1990; Vol. *1*.